

REPORT

## E-Cadherin repression increases amount of cancer stem cells in human A549 lung adenocarcinoma and stimulates tumor growth

M. Farmakovskaya<sup>a,§</sup>, N. Khromova<sup>a,§</sup>, V. Rybko<sup>a</sup>, V. Dugina<sup>b</sup>, B. Kopnin<sup>a</sup>, and P. Kopnin<sup>a</sup>

<sup>a</sup>Blokhin Russian Cancer Research Center, Moscow, Russia; <sup>b</sup>Belozersky Institute of Physico-Chemical Biology, Lomonosov Moscow State University, Moscow, Russia

### ABSTRACT

Here we show that cancer stem cells amount in human lung adenocarcinoma cell line A549 depends on E-cadherin expression. In fact, downregulation of E-cadherin expression enhanced expression of pluripotent genes (*c-MYC*, *NESTIN*, *OCT3/4* and *SOX2*) and enriched cell population with the cells possessing the properties of so-called 'cancer stem cells' via activation of Wnt/ $\beta$ -catenin signaling. Repression of E-cadherin also stimulated cell proliferation and migration *in vitro*, decreased cell amount essential for xenografts formation in nude mice, increased tumors vascularization and growth. On the other hand, E-cadherin upregulation caused opposite effects i.e. diminished the number of cancer stem cells, decreased xenograft vascularization and decelerated tumor growth. Therefore, agents restoring E-cadherin expression may be useful in anticancer therapy.

### ARTICLE HISTORY

Received 7 December 2015  
Revised 9 February 2016  
Accepted 15 February 2016

### KEYWORDS

$\beta$ -catenin; cancer stem cells (CSCs); E-cadherin; tumor progression; wnt-signaling

### Introduction

E-cadherin is a transmembrane calcium-dependent adhesion molecule expressed in almost all epithelial cells. It plays essential roles in embryogenesis and maintenance of adult epithelia, while alterations of its expression/function contributes to tumor development.<sup>1,2</sup> Aberrant adhesion junctions, E-cadherin downregulation or complete shutdown of its expression (through E-cadherin gene mutation, epigenetic or transcriptional silencing, etc.) were found in many human carcinomas. These facts allowed considering it as a tumor suppressor.<sup>3</sup> Inactivating germ-line mutations of *CDH1* gene coding E-cadherin increase the risk of development of familial gastric carcinomas,<sup>4,5</sup> while loss of E-cadherin during tumor progression may result in epithelium to mesenchyme transition (EMT).<sup>6-8</sup> Noteworthy, a correlation between E-cadherin expression and survival of cancer patients was shown.<sup>9-11</sup>

The cells passing through EMT lose polarity, acquire spindle-like shape and enhanced migratory and invasive capacities.<sup>12-14</sup> Nonetheless, some studies showed a crucial necessity in a reverse process – mesenchyme to epithelium transition (MET) when re-expression of E-cadherin was crucial for efficient metastasis formation.<sup>15-17</sup>

During the last few years a connection between EMT and acquisition of so-called [cancer stem cells] (CSCs) phenotype was described.<sup>18-22</sup> According to the CSCs model, heterogeneous cancer cells are arranged in a hierarchical manner with a small cell population on the top harboring tumorigenic capacity. These tumorigenic cells are called CSCs or tumor initiating cells (TICs). It is proposed that they play a

leading role in tumor progression and metastasis while an impact of other cancer cells seems to be less prominent. CSCs could originate from the long-term or transient amplifying normal stem cells<sup>23,24</sup> and possess certain properties, allowing their isolation as a definite minor population in the bulk of tumor cells. They can be both quiescent and capable of self-renewing; they can also contribute to tumor growth by giving rise to cells with high proliferating potential.<sup>25,26</sup> However recent studies revealed a complicated mechanism maintaining a certain ratio of CSCs in the tumor cells population, particularly as a result of conversion of other cancer cells.<sup>27-29</sup>

The ways cancer cell turn into CSCs are poorly studied. It has been shown in many experiments that up- or downregulation of several genes (for example, *TAZ*, *WNT*, *SHH*, *DKK-1*, *PTEN*, *BMI-1*) could influence the proportion of CSCs in cancer cell populations.<sup>30-33</sup> Taking into consideration that disappearance of E-cadherin intercellular adhesions is a major manifestation of EMT,<sup>13,14</sup> that is often accompanied by acquisition of cell features ascribed to CSCs<sup>18-22</sup> we decided to determine whether changes in E-cadherin expression could represent one of the driving forces in acquisition of CSCs phenotype. Previous experimental data concerning this idea were quite controversial. Some results supported this assumption. In fact, it has been shown for breast cancer HMLER and colon cancer SW480 cells that *CDH1* gene knockdown led to enrichment of CD24<sup>-</sup>/CD44<sup>+</sup> cells – a CSCs phenotype for these tumors.<sup>34,35</sup> Moreover, *CDH1* gene downregulation increased tumorigenic potential of HMLER cells<sup>34</sup> – a basic feature of CSCs. On the other hand, there

were reports showing that only E-cadherin-positive prostate cancer cells exhibited a CSCs phenotype, and that its over-expression led to an increase in the proportion of CSCs.<sup>36</sup> Further indirect evidence that E-cadherin can affect CSCs based on our previous results.<sup>37</sup> Inactivation of human endothelial growth factor VEGF-C decreased population of CSCs in colon carcinoma HCT116 and lung carcinoma A549 cells and increased E-cadherin expression was observed.

To assess in more detail the effects of changes in E-cadherin expression on manifestations of CSCs phenotype we constructed lentiviral vectors able to inhibit or increase *CDH1* gene expression and as result created human lung cancer A549 sublines with down- and upregulated E-cadherin.

## Materials and methods

### Cells

Human lung carcinoma A549 cell line (ATCC #CCL-185) expressing *CDH1* or siRNA specific for *CDH1*. For E-cadherin expression cDNA of human *CDH1* (GenBank: Z13009.1; cloned and verified into pBLEc plasmid<sup>38</sup> and kindly provided by Prof. Sergey M. Troyanovsky) was inserted into the lentiviral pLenti6 vector (Invitrogen). For expression of siRNAs specific for *CDH1*, the hairpin structures containing 21-bp sequences corresponding to 5 different parts of *CDH1* mRNA (Fig. 1A) were synthesized and AgeI/EcoRI cloned into the lentiviral pLKO.1-puro vector (Addgene, plasmid #8453). pLKO.1-shGFP-puro targeting eGFP (GenBank Accession No. pEGFP U55761) was used as a control. Oligonucleotides synthesis and DNA sequencing was performed by Evrogen (www.evrogen.com).

The pLenti6 and pLKO lentiviral DNA constructs together with the pΔR8.2 and pVSV-G packaging plasmids were transfected into 293FT cells using TurboFect Transfection Reagent (R0531, Thermo Scientific). Virus-containing supernatants collected 24 to 48 h after transfection and were used to infect recipient A549 cells in the presence of polybrene (8 μg/mL). As hairpin structures sh*CDH1*#4 and sh*CDH1*#5 were the most effective and had similar biological effects, supernatants containing these lentiviruses were combined and applied together. Infected cell cultures were selected for 5–6 d in medium containing 4 mg/ml blasticidin (R210-01, Invitrogen) for pLenti6 constructs or 1 μg/ml puromycin (P8833, Sigma) for pLKO constructs. Cells were cultured in DMEM medium supplemented with 10% fetal bovine serum and penicillin/streptomycin.

### Reverse transcription-PCR assay

Total mRNA was isolated with SV Total RNA Isolation System (Promega) according to the manufacturer's protocols. To detect the corresponding gene expression using endpoint PCR, the following primers and conditions were used:

*E-cadherin*: F 5'-GTCTGTAGGAAGGCACAGCC-3',  
R 5'-TGCAACGTCGTTACGAGTCA-3', 32 amplification cycles;

*c-myc*: F 5'-GGCTTCTCAGAGGCTTGGCGGGAAA-3',  
R 5'-CCTGGGGGATCAAGCGGGAGG-3', 40 amplification cycles;

*Nestin* F 5'-GCGGCTGCGGGCTACTGAAA-3',  
R 5'-ATCCAAGACGCCGGCCCTCT-3', 40 amplification cycles;

*Sox2*: F 5'-TGGACAGTTACGCGCACAT-3',  
R 5'-CGAGTAGGACATGCTGTAGGT-3', 40 amplification cycles;

*Oct3/4*: F 5'-GTGTTTCAGCCAAAAGACCATCT-3',  
R 5'-GGCCTGCATGAGGGTTTCT-3', 40 amplification cycles;

*α-tubulin*: F 5'-GTTGGTCTGGAATTCTGTCAG-3',  
R 5'-AAGAAGTCCAAGCTGGAGTTC-3', 30 amplification cycles;

initial denaturation 95°C 60 s; amplification: denaturation 95°C 30 s, annealing 60°C 30 s (for all primers), extension 72°C 30 s; final extension 5 min at 72°C.

The detection of PCR bands was performed using Chemi-Smart 3000 Imaging System (Vilber Lourmat).

For Real-time qPCR analysis IQ5 Biorad PCR Detection System (Biorad) was used. Real-time PCR was performed using 2.5x SYBR Green real-time PCR mix (Syntol, Russia) according to manufacturer protocol with addition of 0.4 μM of primers (forward, reverse) and 50 ng of cDNA and DEPC-treated water to the final volume of 25 μL. PCR conditions were as follows: 94°C for 5 min, followed by 40 cycles of amplification: 94°C for 10 s, 60°C for 10 s, and 72°C for 20s. For all genes, except *Nestin* (F 5'-CTCCAGAACTCAAGCACC-3', R 5'-TCCTGATTCTCCTCTTCCA-3') and *Sox2* (F 5'-TTCACATGTCCAGCACTACCAGA-3', R 5'-TCA-CATGTGTGAGAGGGGCAGTGTGC-3'), the same primers in qPCR were used. The PCR products were checked for specificity with agarose gel electrophoresis and melt-curve analysis. Data was analyzed with CFX Manager Software (BioRad). *Alpha-tubulin* gene was used for data normalization. Samples were collected from 3 independent cultures. Data was analyzed based on 2-ΔΔCt method.

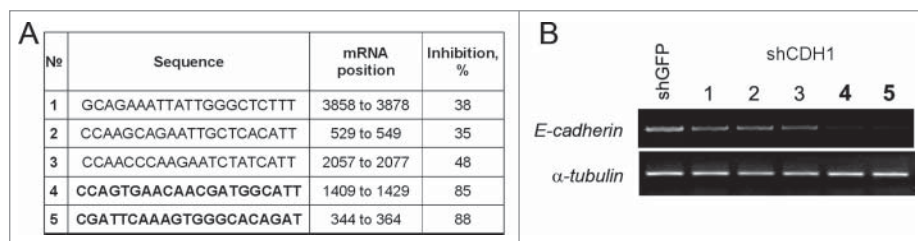


**Figure 1.** Obtaining constructs expressing shRNA specific for *CDH1*. (A) The sequences of 21 nucleotide regions corresponding to the human *CDH1* mRNA (Sequence ID: ref NM\_004360.3), validated as siRNA #4 and #5 (bold) – most effective targets. (B) Effect of transduction of lentiviral constructs pLKO.1-sh*CDH1* on expression of E-cadherin in A549. RT-PCR analysis of *CDH1* expression with corresponding shRNAs (#1–5). *α-tubulin* mRNA was analyzed as loading control.

### **Western blot analysis, total and nuclear protein extract preparation**

was performed as previously described.<sup>39</sup> Primary antibodies specific to E-cadherin (M126, Takara), vimentin (M0725, Dako),  $\beta$ -catenin (M3539, Dako),  $\alpha$ -tubulin (sc-23948, Santa Cruz Biotechnology), histone H3 (9715, Cell Signaling) and Alexa488-conjugated secondary antibodies were used, band detection was performed using variable mode imager Typhoon9410 (GE Healthcare). The quantitation of protein bands was performed using TotalLab v.2.01 software.

### **Immunofluorescent microscopy**

Cells on cover slips were fixed on the fourth day after plating with 1% PFA for 15 min and treated with methanol for 5 min at  $-20^{\circ}\text{C}$ . Cells were incubated with primary (see 2.3) and secondary AlexaFluor594- or Alexa488-conjugated (Invitrogen) antibodies. DAPI (Life technologies) was applied for nuclear staining. Images were acquired using fluorescent Axio-plan 2 microscope and AxioVision (Carl Zeiss Imaging Systems) software.

### **Luciferase reporter assay**

was performed using commercially available Lenti TCF/LEF reporter (Cignal Lenti TCF/LEF Reporter (luc) Kit: CLS-018L, Qiagen) and Steady-Glo Luciferase Assay System (E2510, Promega) according to the manufacturer's protocols; the values were normalized in relation to protein concentration.

### **Boyden chamber cell migration assay**

was performed using transwell Matrigel-coated chambers with  $8\text{-}\mu\text{m}$  pore-size membranes (BD Biosciences) according to manufacturer instructions with  $5 \times 10^4$  A549 cells. The migration activity was quantified by blind counting of the migrated cells of at least 10 fields per chamber.

### **Cell cultures growth rate**

Cells ( $10^4$ ) were plated on the 6-well culture plates and grown without passaging. Cell counts were performed each 48 hours using a hemocytometer (3 wells per point). The measurement proceeded until monolayer formation.

### **FACScan analysis**

Cells were collected from subconfluent culture and the final concentration of  $10^6$  cells/ml in pre-warmed Hank's balanced salt solution containing 2% fetal bovine serum was used. The cells were incubated with 1 mg/ml Rhodamine123 dye (R8004, Sigma) for 30 min in dark at  $37^{\circ}\text{C}$  with intermittent mixing. At the end of the incubation, cells were spun down and washed in cold Hank's balanced salt solution containing 2% fetal bovine serum at  $4^{\circ}\text{C}$  and were labeled with 10mg/ml propidium iodide (P4170, Sigma) to distinguish live from dead cells before analysis. Rhodamine123 staining was detected using a BD

FACSCanto II flow cytometer (BD Biosciences), exciting at 488 nm and detecting Rhodamine123 with a 530/30 broad pass (BP) filter and propidium iodide with a 630/22 BP filter.  $10^7$  events within the live gate were tracked for further analysis using BD FACSDiva Software (BD Biosciences) and WinMDI (Joseph Trotter) software.

### **Clonogenic assay**

200 cells were added to 2,6% methylcellulose (Fluka), mixed with  $2 \times$  DMEM supplemented with 20% fetal bovine serum, plated on non-adherent Petri dishes and cultured at  $37^{\circ}\text{C}$  for 14 d. The colonies were stained with crystal violet and incubated at  $4^{\circ}\text{C}$  overnight. Colonies were counted with TotalLab v.2.01 software, module Colony Counter (Nonlinear Dynamics).

### **Nude mice assay**

D2 x J nude mice (10 animals for each experimental group) were inoculated subcutaneously with dosages of cells suspended in 100 ml of PBS:  $10^6$ ;  $0,5 \times 10^6$ ;  $0,25 \times 10^6$ ;  $0,125 \times 10^6$  and  $0,005 \times 10^6$ . Tumor sizes were measured every 3 d and their volumes were calculated as  $(\text{width}^2) \times (\text{length}) \times 0,5$ . After 25 d of observation, explanted tumors were isolated and analyzed immunohistochemically. These experiments were repeated 3 times to confirm the results.

The animal experimental protocols were approved by the Committee for Ethics of Animal Experimentation and the experiments were conducted in accordance with the Guidelines for Animal Experiments in Blokhin Memorial Russian Cancer Research Center.

### **Immunohistochemistry**

Antigen retrieval was achieved by heating ( $95^{\circ}\text{C}$ ) of the sections in target retrieval solution pH 6.0 (S1699, Dako) for 40 min. The sections were incubated with primary antibodies to CD34 (553731, BD Biosciences PharMingen) at room temperature for 1 hour, followed by incubations with biotin-conjugated (559286 BD Biosciences PharMingen) secondary antibodies for 30 min at room temperature. To identify the target Streptavidin-HRP (Dako) was added for 15 min at room temperature. The reactivity was visualized with DAB+ (diaminobenzidine) (K3468, Dako) according to the manufacturer's instructions. Sections were counterstained with Mayer's hematoxylin and mounted. Vessels and capillaries, identified by positive staining for CD34 and appropriate morphology, were counted. Angiogenic properties were scored as average number of relatively large microvessels (the size of lumens  $P > 100 \mu\text{m}$  in length). On average, immunohistochemistry quantification was performed by taking pictures from maximum possible fields per tumor, at least 15 fields of vision per tumor type, and imaging at least 6 tumors per cell subline type using AxioVision software (Carl Zeiss Imaging Systems).

## Statistical analysis

All experiments were performed in triplicate and data are expressed as mean  $\pm$  SD, as indicated in figure legends. Statistical analysis was performed using unpaired Student's t test. P values  $\leq 0.05$  were considered to be significant. The GraphPad Prism statistical software package ver. 5.01 was used.

## Results

To investigate the influence of E-cadherin expression on properties of lung adenocarcinoma cells and possible role in

cancer stem cell phenotype formation we obtained A549 derivatives with overexpressed or silenced E-cadherin. For E-cadherin overexpression ORF of human *CDH1* gene was cloned into modified lentiviral vector pLenti6. The vector has the CMV promoter for driving constitutive expression of the target gene and the blasticidin selection marker for stable selection in mammalian cells. Based on MISSION<sup>®</sup> shRNA Library (Sigma-Aldrich) 5 validated siRNA targets of human *CDH1* mRNA were tested on A549 cells and 2 most effective targets (#4,5 Fig. 1) were cloned into pLKO.1 lentiviral vector for siRNA expression for stable E-Cadherin repression (Fig. 1).

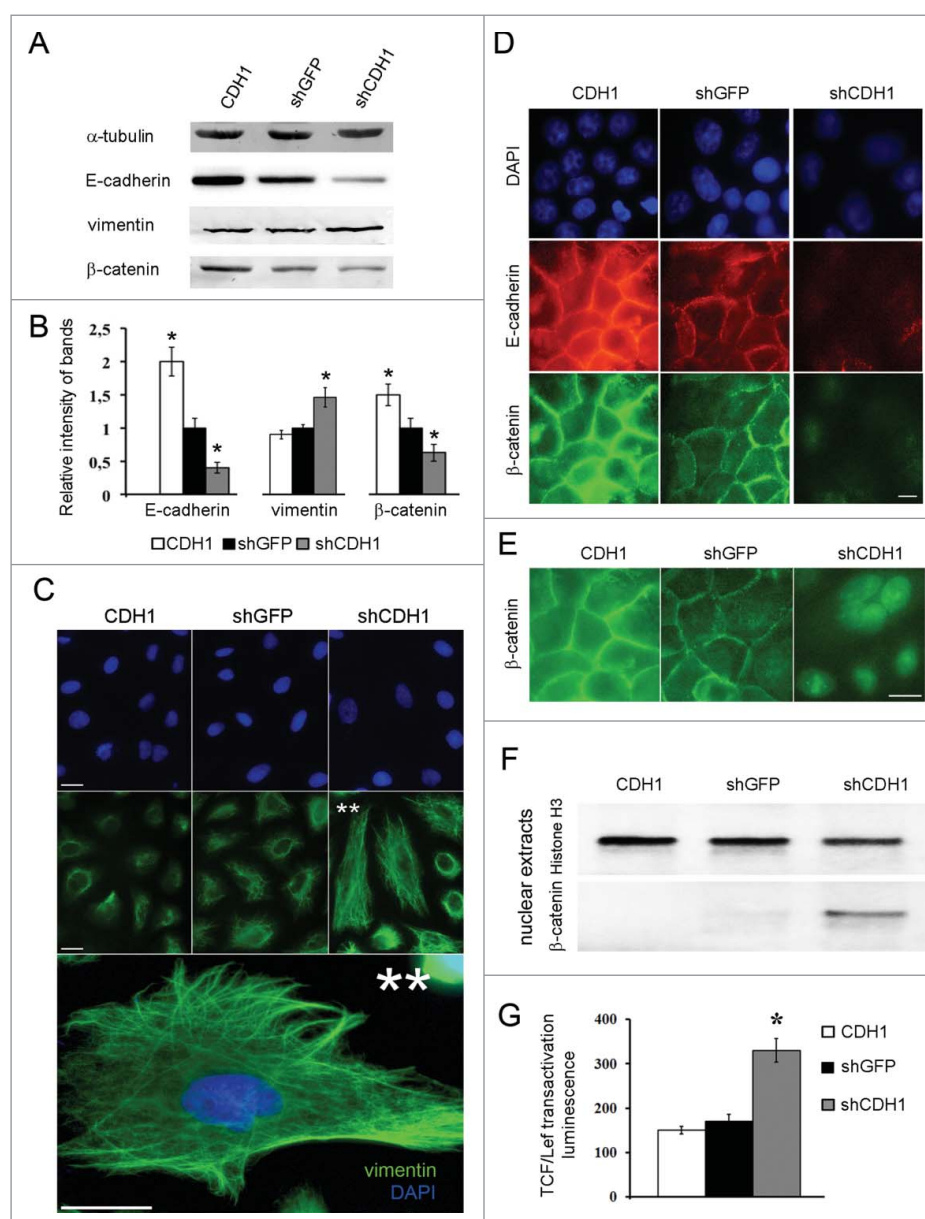


**Figure 2.** Effects of E-cadherin expression alterations on morphology features and activation of Wnt/ $\beta$ -catenin signaling pathway in A549 cells. (A) A representative Western blot analysis of E-cadherin, vimentin and  $\beta$ -catenin expression in A549 cell sublines.  $\alpha$ -tubulin was analyzed as loading control. (B) Average results of E-cadherin, vimentin and  $\beta$ -catenin bands densitometry analysis normalized by tubulin expression of 3 independent experiments (Mean  $\pm$  SD, \* -  $p \leq 0.05$ ). (C) Immunofluorescent staining of A549 cell sublines with antibodies to vimentin. Bars 5  $\mu$ m. \*\* - Enlarged A549shCDH1 cells with well-detected vimentin filaments. (D) Immunofluorescent staining of A549 cell sublines stained with E-cadherin and  $\beta$ -catenin antibodies. Bars 5  $\mu$ m. (E) Enlarged and strongly enhanced immunofluorescent images of  $\beta$ -catenin staining of A549 cell sublines for nuclear  $\beta$ -catenin detection. Bars 5  $\mu$ m. (F) Nuclear extracts Western blot analysis of  $\beta$ -catenin in A549 cell sublines. Histone H3 was used as loading control. (G) The reporter construct expressing luciferase gene under control of TCF/Lef was introduced into A549 cell sublines, luciferase activity was measured in 3 experiments; average data are presented (Mean  $\pm$  SD, \*  $p \leq 0.05$ ).



A549 cells with silenced E-cadherin expression acquired a more mesenchymal phenotype while cells with overexpressed E-cadherin looked more epithelial and had enhanced tight junctions. Inactivation of E-cadherin was accompanied with a slight increase of total vimentin levels (Fig. 2A). To prove the fact, since changes of vimentin protein amounts were not prominent upon E-cadherin up- and downregulation, A549 cells were infected 3 times independently and independent western blots were accomplished. Average densitometry results confirmed slight increasing of vimentin amounts (up to 1.5–2 times) caused by *CDH1* repression (Fig. 2B). Despite this fact, significant vimentin filaments formation in cells with downregulated E-cadherin expression was observed (Fig. 2C). E-cadherin downregulation caused disappearance of E-cadherin junctions, decrease of total  $\beta$ -catenin amount with its' translocation and slight accumulation in the nuclei (Fig. 2D). As nuclear  $\beta$ -catenin accumulation was not prominent and was detected with strong fluorescent enhancement (Fig. 2E) we analyzed  $\beta$ -catenin content in the nuclear extracts. Nuclear  $\beta$ -catenin was detected only in cells with repressed *CDH1* gene (Fig. 2F). Histone H3 as a nuclear marker was used. Nuclear translocation of  $\beta$ -catenin is usually accompanied by its transcriptional function induction, so we tested the Wnt/ $\beta$ -catenin signaling pathway activation upon changes of E-cadherin expression. Using luciferase TCF/Lef-dependent reporter (Qia-gen) we have shown that E-cadherin repression led to activation of TCF/Lef-dependent transcription (Fig. 2G). As the conserved Wnt/ $\beta$ -catenin pathway regulates stem cell pluripotency and cell fate decisions during development,<sup>36,40–42</sup> we analyzed mRNA levels of some of the pluripotency genes.

Increased transcription of *c-MYC*, *NESTIN*, *OCT3/4* and *SOX2* genes was detected in A549 cells with silenced *CDH1* using end-point PCR (Fig. 3A) and confirmed by Real-time qPCR (Fig. 3B). As increased expression of these genes is connected not only with “normal” stem cells but is also observed in “cancer” stem cells,<sup>42–44</sup> we also studied the influence of E-cadherin expression alterations on the proportion of cells with the CSCs traits in A549 cell sublines. For this purpose generally accepted approaches were used. Firstly we investigated the activity of ABC-transporters analyzing Rhodamine123 content in A549 cells with modified E-cadherin expression using FACS flow cytometry. Amount of side-population cells with enhanced ABC-transporter activity, one of the features of CSCs,<sup>21,44</sup> was increased in the A549 subline with inactivated E-cadherin

(sh*CDH1*) and decreased in the subline with overexpressed E-cadherin (*CDH1*) (Fig. 4A). Then we tested cell abilities to form colonies in semisolid medium under non-adherent conditions. Subline with repressed E-cadherin formed up to 4 times more colonies than control A549 cells and more than 10 times compared with overexpressed E-cadherin subline (Fig. 4B). Also A549-sh*CDH1*-formed colonies had noticeably larger size. In addition, more mesenchymal cells with downregulated E-cadherin demonstrated increased migration and invasive activities *in vitro*, when Boyden chamber assay with matrigel-coated filters were used. Upregulation of E-cadherin diminished these properties (Fig. 4C).

The main trait of CSCs is tumorigenic ability in nude mice and injectable cell dose threshold is a very important characteristic.<sup>44</sup> In fact, tumorigenic dosage for cells with overexpressed *CDH1* was increased (Table 1), while sh*CDH1* A549 derivatives needed less cells for tumor formation. All these experiments indicate on the dependence of CSCs population on the levels of E-cadherin in A549 cells.

Besides enhancing CSCs properties, E-cadherin inactivation enhanced A549 cell proliferation *in vitro* (Fig. 5A) and stimulated vascularization and growth of tumor xenografts in nude mice (Fig. 5B,C). On the other hand, E-cadherin upregulation reduced the number of blood vessels and decelerated tumor growth (Fig. 5B,C).

It should be stressed, that A549 cells expressing sh*GFP* was used as control in all experiments, and they did not differ from parental A549 culture in any analyzed characteristics or tests and showed similar results.

## Discussion

To ascertain the effects of E-cadherin expression modulation on acquisition of cancer stem cell phenotype we generated the A549 human non-small-cell lung carcinoma (NSCLC) cells with different levels of E-cadherin expression: E-cadherin<sup>high</sup> and E-cadherin<sup>low</sup>. We noticed that E-cadherin<sup>low</sup> cells lost epithelial and acquired some mesenchymal features, such as slight increase of vimentin expression accompanied by twisted and strengthened vimentin filament network and enhanced migratory capacity. These findings confirmed that E-cadherin<sup>low</sup> cell lines could acquire some features of epithelial-to-mesenchymal

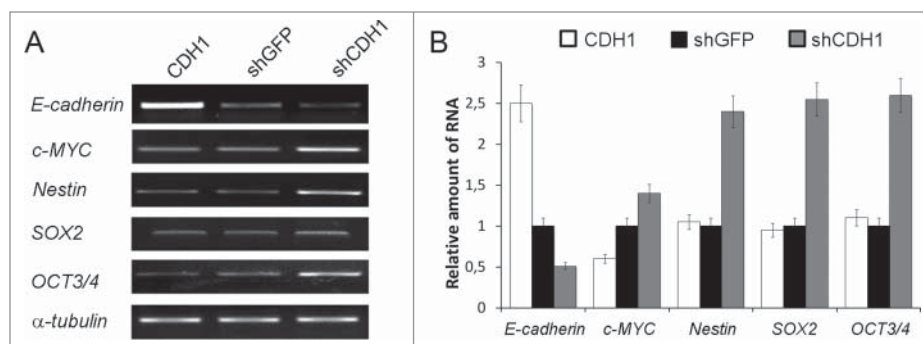


**Figure 3.** Effect of *E-cadherin* expression alterations on the pluripotency genes expression. (A) The result of one of the representative End-point PCR experiments.  $\alpha$ -tubulin mRNA was analyzed as loading control. (B) Relative quantities of mRNAs estimated by Real-time qPCR.  $\alpha$ -tubulin gene was used for data normalization (Mean  $\pm$  SD).

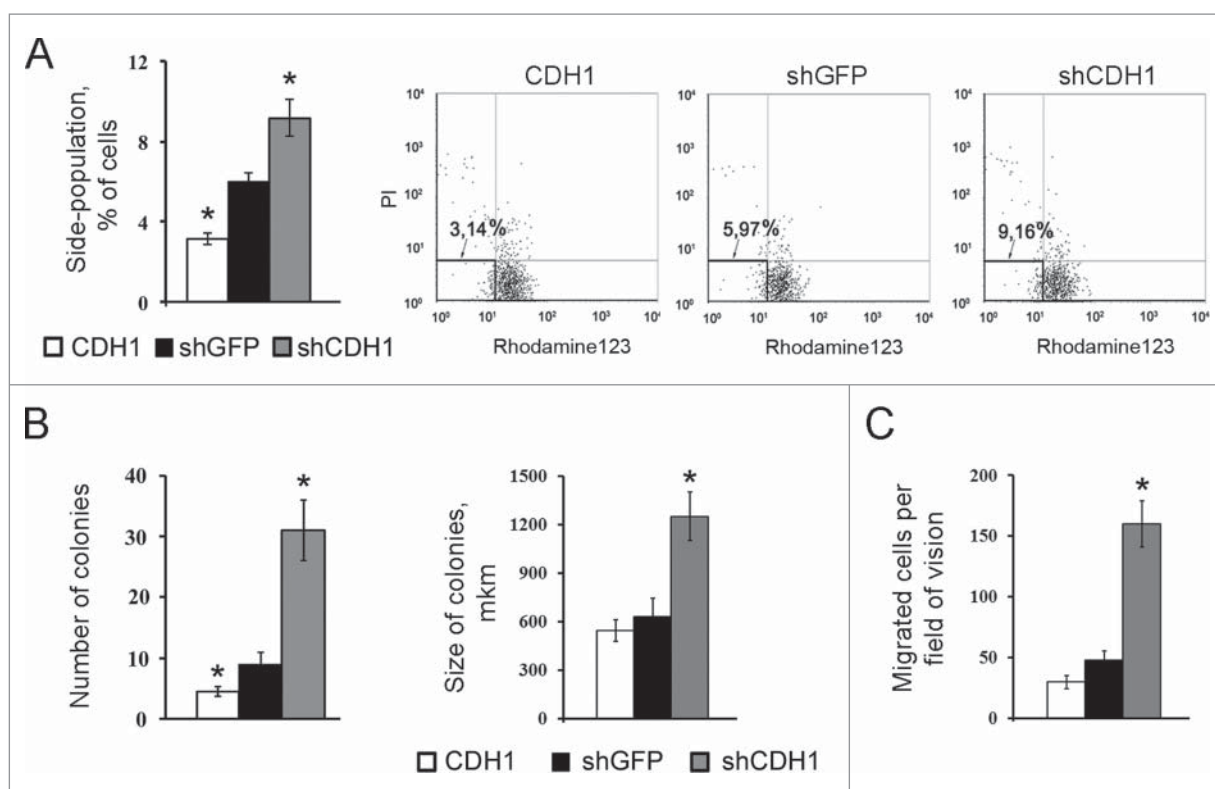


**Figure 4.** The effect of E-cadherin expression alterations on the percentage of cells with the CSCs features in A549 cell populations. (A) ABC-transporters activity by analysis of Rhodamine123 content in A549 sublines using flow cytometry. *Left panel* – results of quantitative estimation of side-population cells, (Mean  $\pm$  SD, \*  $p \leq 0,05$ ). *Right panel* – distribution of  $10^7$  cells according to their fluorescence; side populations of weakly fluorescent cells were counted in the left lower quadrants. (B) Clonogenic capacity of A549 cell sublines in non-adherent conditions. Results of quantitative estimation of the colony number (*left panel*) and colony size (*right panel*), (Mean  $\pm$  SD, \*  $p \leq 0,05$ ). (C) Invasion of A549 sublines in Boyden chambers through matrigel-coated membranes (Mean  $\pm$  SD, \*  $p \leq 0,05$ ).

transition (EMT) whereas E-cadherin<sup>high</sup> cell lines and control cells retained epithelial phenotype.

As far as we noticed that cell lines with downregulated E-cadherin changed their morphology we examined how changes in E-cadherin expression would affect growth kinetics *in vitro* and *in vivo*. E-cadherin upregulation caused some deceleration of growth rate both *in vitro* and *in vivo*, while E-cadherin downregulation increased the growth rate, and the effect was particularly strong *in vivo*. In fact, xenografts with reduced *CDH1* expression showed approximately 2-fold increases in final tumors volumes. As tumor vascularization is considered to be a major limiting factor of tumor development<sup>45,46</sup> we examined the density of blood vessels in tumor xenografts. We demonstrated that the density of large vessels (larger than 100  $\mu$ m) was significantly increased in E-cadherin<sup>low</sup> tumors at least partially explaining their faster growth and larger sizes.

**Table 1.** The effect of E-cadherin expression alterations on tumorigenic ability of A549 cells.

Sublines	Tumorigenicity (%)*				
	$1 \times 10^6$	$0,5 \times 10^6$	$0,25 \times 10^6$	$0,125 \times 10^6$	$0,05 \times 10^6$
<i>CDH1</i>	100%	100%	50%	0%	0%
<i>shGFP</i>	100%	100%	75%	15%	0%
<i>shCDH1</i>	100%	100%	100%	50%	10%

\*Number of mice with tumors/total number of mice with injected cells.

Conducting xenograft assay we noticed that the threshold cell dose for E-cadherin<sup>low</sup> cell subline was significantly lower than that for control cell line while on the contrary the threshold dose for E-cadherin<sup>high</sup> cells was higher than for control cell lines. That is why we proposed that E-cadherin downregulation could lead to an increase of the proportion of CSCs as the ability to form new tumors is considered to be the main characteristic of CSCs. To prove this we performed a series of experiments that were believed to serve as a so-called “gold standard” for assessing the percentage of the CSCs: determined the cell dose threshold for tumor formation in nude mice; detected cells that effectively excluded Rhodamine123 and assessed colony formation in semisolid medium.<sup>44</sup> As the result of all 3 tests we proved that E-cadherin<sup>low</sup> A549 cells were enriched with CSCs, while in E-cadherin<sup>high</sup> cells the percentage of CSCs was reduced. This allows us to suggest that loss of E-cadherin expression could lead to the acquisition of CSCs phenotype.

To obtain more characteristics for cells with altered E-cadherin expression we analyzed expression of some stem cell markers, such as *OCT3/4*, *SOX2*, *Nestin* and the oncogene *c-MYC*. We observed elevated levels of mRNAs of all these genes in E-cadherin<sup>low</sup> cells. So, downregulation of E-cadherin results in elevation of genes that are believed to maintain stem state of the cell. We suppose that E-cadherin downregulation might promote the increased expression of stem-maintaining transcriptional factors Oct3/4 and SOX2, which in turn could play a role in acquisition of cancer stem cell features. The influence

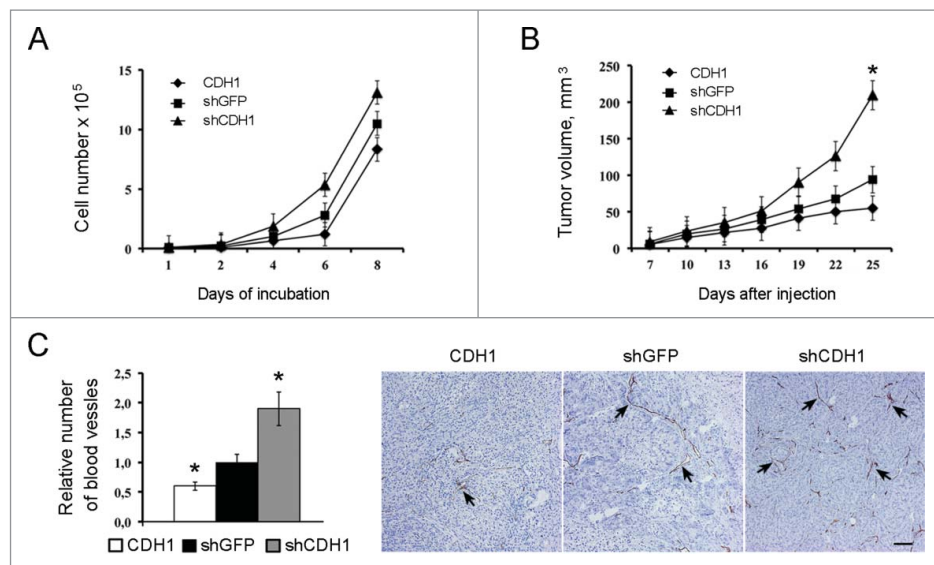


**Figure 5.** The effect of E-cadherin expression alterations on the growth kinetics of A549 cells *in vitro*, *in vivo* and on the xenografts vascularization. (A) Proliferation dynamics of cells. Typical result of one of 3 experiments is shown (Mean  $\pm$  SD). (B) Dynamics of xenografts growth after subcutaneous injection (10 mice per group) of A549 cells. Typical result of one of 3 experiments is given (Mean  $\pm$  SD, \*  $p \leq 0,05$ ). (C) Immunohistochemical analysis for CD34 of A549 xenografts with modulated E-cadherin expression. *Left panel* - quantitative estimation of CD34-positive blood vessels larger 100  $\mu\text{m}$ . 20–25 fields of view in each experimental group were analyzed (Mean  $\pm$  SD, \*  $p \leq 0,05$ ). *Right panel* - representative fields of view for each experimental group. Spikes – CD34-positive structures. Bars 100  $\mu\text{m}$ .

of E-cadherin expression on CSCs phenotype is summarized on the scheme (Fig. 6). A549 cells were additionally cloned and after several passages different clones showed similar, between themselves and initial cell culture, characteristics in CSCs functional tests (data not shown). These results are in accordance with the hypothesis of dynamic CSCs status, dependent on different intra- and extra-cellular conditions.<sup>26–29</sup>

Taken together the results of our work show that downregulation of *CDH1* increased while its upregulation decreased various cell features ascribed to CSCs, including tumorigenic potential. This allowed considering changes in E-cadherin

intercellular adhesions as one of the molecular determinants responsible for dynamic increase/decrease of manifestations of CSCs phenotype. Since CSCs are the driving force for tumor progression and metastasis, elimination of this tumor cell population seems to be extremely important in anticancer therapy. We believe that restoring E-cadherin function could be relatively safe in this respect.

## Disclosure of potential conflicts of interest

No potential conflicts of interest were disclosed.

## Funding

KPB is grateful to the Russian Science Foundation (RSCF), grant No. 14-15-00467 for support.

## References

- [1] Stemmler MP. Cadherins in development and cancer. *Mol Biosyst* 2008; 4(8):835–50; PMID:18633485; <http://dx.doi.org/10.1039/b719215k>
- [2] van Roy F, Berx G. The cell-cell adhesion molecule E-cadherin. *Cell Mol Life Sci*. 2008; 65(23):3756–88; PMID:18726070; <http://dx.doi.org/10.1007/s00018-008-8281-1>
- [3] Rodriguez FJ, Lewis-Tuffin LJ, Anastasiadis PZ. E-cadherin's dark side: possible role in tumor progression. *Biochim Biophys Acta* 2012; 1826(1):23–31; PMID:22440943
- [4] Chun N, Ford JM. Genetic testing by cancer site: stomach. *Cancer J* 2012; 18(4):355–63; PMID:22846738; <http://dx.doi.org/10.1097/PPO.0b013e31826246dc>
- [5] Corso G, Marrelli D, Pascale V, Vindigni C, Roviello F. Frequency of *CDH1* germline mutations in gastric carcinoma coming from high- and low-risk areas: metanalysis and systematic review of the literature. *BMC Cancer* 2012; 12:8; PMID:22225527; <http://dx.doi.org/10.1186/1471-2407-12-8>
- [6] Spaderna S, Schmalhofer O, Hlubek F, Jung A, Kirchner T, Brabletz T. Epithelial-mesenchymal and mesenchymal-epithelial transitions

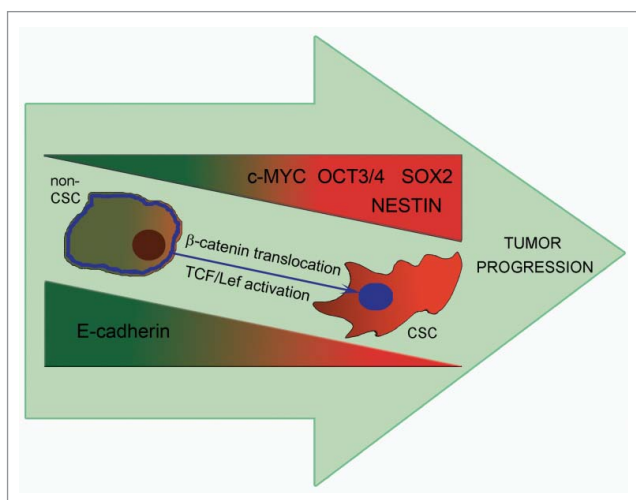


**Figure 6.** Upon tumor progression E-cadherin downregulation leads to an increase of the proportion of CSCs and acquisition of the ability to form secondary foci of tumor growth. E-cadherin repression results in elevation of genes maintaining stemness – Oct3/4, SOX2, Nestin and c-Myc playing a role in acquisition of CSCs features. A possible mechanism for the enhancement of CSCs properties may be the translocation of  $\beta$ -catenin to the nucleus and activation of the Wnt/ $\beta$ -catenin pathway (partly through c-MYC increased transcription).

- during cancer progression. *Verh Dtsch Ges Pathol* 2007; 91:21-8; PMID:18314592
- [7] Schmalhofer O, Brabletz S, Brabletz T. E-cadherin, beta-catenin, and ZEB1 in malignant progression of cancer. *Cancer Metastasis Rev* 2009; 28(1-2):151-66; PMID:19153669; <http://dx.doi.org/10.1007/s10555-008-9179-y>
- [8] Yilmaz M, Christofori G. Mechanisms of motility in metastasizing cells. *Mol Cancer Res* 2010; 8(5):629-42; PMID:20460404; <http://dx.doi.org/10.1158/1541-7786.MCR-10-0139>
- [9] Kim A, Bae YK, Gu MJ, Kim JY, Jang KY, Bae HI, Lee HJ, Hong SM. Epithelial-mesenchymal transition phenotype is associated with patient survival in small intestinal adenocarcinoma. *Pathology* 2013; 45(6):567-73; PMID:24018801; <http://dx.doi.org/10.1097/PAT.0b013e3283650bab>
- [10] Bae YK, Choi JE, Kang SH, Lee SJ. Epithelial-mesenchymal transition phenotype is associated with clinicopathological factors that indicate aggressive biological behavior and poor clinical outcomes in invasive breast cancer. *J Breast Cancer* 2015; 18(3):256-63; PMID:26472976; <http://dx.doi.org/10.4048/jbc.2015.18.3.256>
- [11] Kobayashi H, Sugimoto H, Onishi S, Nakano K. Novel biomarker candidates for the diagnosis of ovarian clear cell carcinoma. *Oncol Lett* 2015; 10(2):612-18; PMID:26622542
- [12] Lee JM, Dedhar S, Kalluri R, Thompson EW. The epithelial-mesenchymal transition: new insights in signaling, development, and disease. *J Cell Biol* 2006; 172(7):973-81; PMID:16567498; <http://dx.doi.org/10.1083/jcb.200601018>
- [13] Thiery JP, Acloque H, Huang RY, Nieto MA. Epithelial-mesenchymal transitions in development and disease. *Cell* 2009; 139(5):871-90; PMID:19945376; <http://dx.doi.org/10.1016/j.cell.2009.11.007>
- [14] Kalluri R, Weinberg RA. The basics of epithelial-mesenchymal transition. *J Clin Invest* 2009; 119(6):1420-8; PMID:19487818; <http://dx.doi.org/10.1172/JCI39104>
- [15] Yu M, Bardia A, Wittner BS, Stott SL, Smas ME, Ting DT, Isakoff SJ, Ciciliano JC, Wells MN, Shah AM, et al. Circulating breast tumor cells exhibit dynamic changes in epithelial and mesenchymal composition. *Science* 2013; 339(6119):580-4; PMID:23372014; <http://dx.doi.org/10.1126/science.1228522>
- [16] Thiery JP, Lim CT. Tumor dissemination: an EMT affair. *Cancer Cell* 2013; 23(3):272-3; PMID:23518345; <http://dx.doi.org/10.1016/j.ccr.2013.03.004>
- [17] Liu S, Cong Y, Wang D, Sun Y, Deng L, Liu Y, Martin-Trevino R, Shang L, McDermott SP, Landis MD, et al. Breast cancer stem cells transition between epithelial and mesenchymal states reflective of their normal counterparts. *Stem Cell Reports* 2013; 2(1):78-91; PMID:24511467; <http://dx.doi.org/10.1016/j.stemcr.2013.11.009>
- [18] Mani SA, Guo W, Liao MJ, Eaton EN, Ayyanan A, Zhou AY, Brooks M, Reinhard F, Zhang CC, Shipitsin M, et al. The epithelial-mesenchymal transition generates cells with properties of stem cells. *Cell* 2008; 133(4):704-15; PMID:18485877; <http://dx.doi.org/10.1016/j.cell.2008.03.027>
- [19] Abell AN, Johnson GL. Implications of mesenchymal cells in cancer stem cell populations: relevance to EMT. *Curr Pathobiol Rep* 2014; 2(1):21-26; PMID:25530923; <http://dx.doi.org/10.1007/s40139-013-0034-7>
- [20] Polyak K, Weinberg RA. Transitions between epithelial and mesenchymal states: acquisition of malignant and stem cell traits. *Nat Rev Cancer* 2009; 9(4):265-73; PMID:19262571; <http://dx.doi.org/10.1038/nrc2620>
- [21] Singh A, Settleman J. EMT, cancer stem cells and drug resistance: an emerging axis of evil in the war on cancer. *Oncogene* 2010; 29(34):4741-51; PMID:20531305; <http://dx.doi.org/10.1038/onc.2010.215>
- [22] Liu X, Fan D. The epithelial-mesenchymal transition and cancer stem cells: functional and mechanistic links. *Curr Pharm Des* 2015; 21(10):1279-91; PMID:25506898; <http://dx.doi.org/10.2174/1381612821666141211115611>
- [23] Reya T, Morrison SJ, Clarke MF, Weissman IL. Stem cells, cancer, and cancer stem cells. *Nature* 2001; 414(6859):105-11; PMID:11689955; <http://dx.doi.org/10.1038/35102167>
- [24] Scheel C, Weinberg RA. Cancer stem cells and epithelial-mesenchymal transition: concepts and molecular links. *Semin Cancer Biol* 2012; 22(5-6):396-403; PMID:22554795; <http://dx.doi.org/10.1016/j.semcancer.2012.04.001>
- [25] Visvader JE, Lindeman GJ. Cancer stem cells in solid tumours: accumulating evidence and unresolved questions. *Nat Rev Cancer* 2008; 8(10):755-68; PMID:18784658; <http://dx.doi.org/10.1038/nrc2499>
- [26] Gupta PB, Chaffer CL, Weinberg RA. Cancer stem cells: mirage or reality? *Nat Med* 2009; 15(9):1010-2; PMID:19734877; <http://dx.doi.org/10.1038/nm0909-1010>
- [27] Gupta PB, Fillmore CM, Jiang G, Shapira SD, Tao K, Kuperwasser C, Lander ES. Stochastic state transitions give rise to phenotypic equilibrium in populations of cancer cells. *Cell* 2011; 146(4):633-44; PMID:21854987; <http://dx.doi.org/10.1016/j.cell.2011.07.026>
- [28] Chaffer CL, Brueckmann I, Scheel C, Kaestli AJ, Wiggins PA, Rodrigues LO, Brooks M, Reinhardt F, Su Y, Polyak K, et al. Normal and neoplastic nonstem cells can spontaneously convert to a stem-like state. *Proc Natl Acad Sci U S A* 2011; 108(19):7950-5; PMID:21498687; <http://dx.doi.org/10.1073/pnas.1102454108>
- [29] Marjanovic ND, Weinberg RA, Chaffer CL. Cell plasticity and heterogeneity in cancer. *Clin Chem* 2013; 59(1):168-79; PMID:23220226; <http://dx.doi.org/10.1373/clinchem.2012.184655>
- [30] Cordenonsi M, Zanconato F, Azzolin L, Forcato M, Rosato A, Frasson C, Inui M, Montagner M, Parenti AR, Poletti A, et al. The Hippo transducer TAZ confers cancer stem cell-related traits on breast cancer cells. *Cell* 2011; 147(4):759-72; PMID:22078877; <http://dx.doi.org/10.1016/j.cell.2011.09.048>
- [31] Cai C, Zhu X. The Wnt/ $\beta$ -catenin pathway regulates self-renewal of cancer stem-like cells in human gastric cancer. *Mol Med Rep* 2012; 5(5):1191-6; PMID:22367735
- [32] Liu S, Dontu G, Mantle ID, Patel S, Ahn NS, Jackson KW, Suri P, Wicha MS. Hedgehog signaling and Bmi-1 regulate self-renewal of normal and malignant human mammary stem cells. *Cancer Res* 2006; 66(12):6063-71; PMID:16778178; <http://dx.doi.org/10.1158/0008-5472.CAN-06-0054>
- [33] Korkaya H, Paulson A, Charafe-Jauffret E, Ginestier C, Brown M, Dutcher J, Clouthier SG, Wicha MS. Regulation of mammary stem/progenitor cells by PTEN/Akt/ $\beta$ -catenin signaling. *PLoS Biol* 2009; 7(6):e1000121; PMID:19492080; <http://dx.doi.org/10.1371/journal.pbio.1000121>
- [34] Gupta PB, Onder TT, Jiang G, Tao K, Kuperwasser C, Weinberg RA, Lander ES. Identification of selective inhibitors of cancer stem cells by high-throughput screening. *Cell* 2009; 138(4):645-59; PMID:19682730; <http://dx.doi.org/10.1016/j.cell.2009.06.034>
- [35] Ye J, Wu D, Shen J, Wu P, Ni C, Chen J, Zhao J, Zhang T, Wang X, Huang J. Enrichment of colorectal cancer stem cells through epithelial-mesenchymal transition via CDH1 knockdown. *Mol Med Rep* 2012; 6(3):507-12; PMID:22684815
- [36] Bae KM, Su Z, Frye C, McClellan S, Allan RW, Andrejewski JT, Kelley V, Jorgensen M, Steindler DA, Vieweg J, et al. Expression of pluripotent stem cell reprogramming factors by prostate tumor initiating cells. *J Urol* 2010; 183(5):2045-53; PMID:20303530; <http://dx.doi.org/10.1016/j.juro.2009.12.092>
- [37] Khromova N, Kopnin P, Rybko V, Kopnin BP. Downregulation of VEGF-C expression in lung and colon cancer cells decelerates tumor growth and inhibits metastasis via multiple mechanisms. *Oncogene* 2012; 31(11):1389-97; PMID:21804602; <http://dx.doi.org/10.1038/onc.2011.330>
- [38] Chitaev NA, Troyanovsky SM. Adhesive but not lateral E-cadherin complexes require calcium and catenins for their formation. *J Cell Biol* 1998; 142(3):837-46; PMID:9700170; <http://dx.doi.org/10.1083/jcb.142.3.837>
- [39] Zamkova M, Khromova N, Kopnin BP, Kopnin P. Ras-induced ROS upregulation affecting cell proliferation is connected with cell type-specific alterations of HSF1/SEN3/p21Cip1/WAF1 pathways. *Cell Cycle* 2013; 12(5):826-36; PMID:23388456; <http://dx.doi.org/10.4161/cc.23723>
- [40] Ying L, Mills JA, French DL, Gadue P. OCT4 coordinates with WNT signaling to pre-pattern chromatin at the SOX17 locus during human ES cell differentiation into definitive endoderm. *Stem Cell Reports* 2015; 5(4):490-8; PMID:26411902; <http://dx.doi.org/10.1016/j.stemcr.2015.08.014>



- [41] Zhang P, Chang WH, Fong B, Gao F, Liu C, Al Alam D, Bellusci S, Lu W. Regulation of induced pluripotent stem (iPS) cell induction by Wnt/ $\beta$ -catenin signaling. *J Biol Chem* 2014; 289(13):9221-32; PMID:24482235; <http://dx.doi.org/10.1074/jbc.M113.542845>
- [42] Yi XJ, Zhao YH, Qiao LX, Jin CL, Tian J, Li QS. Aberrant Wnt/ $\beta$ -catenin signaling and elevated expression of stem cell proteins are associated with osteosarcoma side population cells of high tumorigenicity. *Mol Med Rep* 2015; 12(4):5042-8; PMID:26134785
- [43] Dahlrot RH, Hermansen SK, Hansen S, Kristensen BW. What is the clinical value of cancer stem cell markers in gliomas? *Int J Clin Exp Pathol* 2013; 6(3):334-48; PMID:23412423
- [44] Richard V, Nair MG, Santhosh Kumar TR, Pillai MR. Side population cells as prototype of chemoresistant, tumor-initiating cells. *Biomed Res Int* 2013; 2013:517237; PMID:24294611; <http://dx.doi.org/10.1155/2013/517237>
- [45] Adams RH, Alitalo K. Molecular regulation of angiogenesis and lymphangiogenesis. *Nat Rev Mol Cell Biol* 2007; 8(6):464-78; PMID:17522591; <http://dx.doi.org/10.1038/nrm2183>
- [46] Khromova NV, Kopnin PB, Stepanova EV, Agapova LS, Kopnin BP. p53 hot-spot mutants increase tumor vascularization via ROS-mediated activation of the HIF1/VEGF-A pathway. *Cancer Lett* 2009; 276(2):143-51; PMID:19091459; <http://dx.doi.org/10.1016/j.canlet.2008.10.049>